Substrate surface corrugation effects on the electronic transport in graphene nanoribbons

Shoeib Babaee Touski and Mahdi Pourfath

Citation: Applied Physics Letters **103**, 143506 (2013); doi: 10.1063/1.4824362
View online: http://dx.doi.org/10.1063/1.4824362
View Table of Contents: http://scitation.aip.org/content/aip/journal/apl/103/14?ver=pdfcov
Published by the AIP Publishing

Substrate surface corrugation effects on the electronic transport in graphene nanoribbons

Shoeib Babaee Touski[1] and Mahdi Pourfath[1,2,a)]
[1]*School of Electrical and Computer Engineering, University of Tehran, P.O. Box 14395-515, Tehran, Iran*
[2]*Institute for Microelectronics, TU Wien, Gusshausstrasse 27-29/E360, 1040 Vienna, Austria*

(Received 30 April 2013; accepted 22 September 2013; published online 3 October 2013)

In this work, the electronic transport in armchair graphene nanoribbons in the presence of surface corrugation is studied. The non-equilibrium Green's function along with tight-binding model for describing the electronic band structure is employed to investigate the electronic properties of graphene nanoribbons. The effects of surface corrugation parameters, such as corrugation amplitude and correlation length, on the electronic properties of the graphene nanoribbons are studied. The mean free path of carriers is extracted and its dependency on the corrugation amplitude and correlation length is investigated. © *2013 AIP Publishing LLC*. [http://dx.doi.org/10.1063/1.4824362]

Graphene has attracted much attention due to its unique electronic, physical, and mechanical properties. Graphene should be placed on a substrate to be usable for electronic applications. Scattering of carriers due to charged impurities and surface corrugation of the substrate surface, however, can degrade the electronic properties of graphene.[1,2] In particular, microscopic corrugations have been observed both on suspended[3] and supported[4–7] graphene sheets. This rippling has been invoked to explain the thermodynamic stability of free-standing graphene sheets.[8] To use graphene for building electronic devices, it should be placed on a substrate. In principle, the underlying substrate has always a degree of surface corrugation, which depends on the material type and the applied polishing method. Surface corrugation affects the surface morphology and can reduce the mobility even further.[9]

When graphene is placed on a substrate, it follows the ripples of the substrate surface[10] (see Fig. 1), where such ripples induce significant stress in the graphene sheet.[2] The height of the surface corrugation approximately varies between 25 pm for mica[4] and 300 pm for SiO_2,[5,6] see Table I. Although the surface of mica is much smoother than that of SiO_2, but SiO_2 is a more common material for semiconductor industries. Modeling surface corrugation with a simple sinusoidal function, Costamagna *et al.*[11] have shown that surface corrugation can induce an electronic band-gap in metallic armchair graphene nanoribbons (AGNRs). In this work, however, by employing an accurate statistical description of the surface corrugation, the role of corrugation on the mobility and mean free paths (MFPs) of carriers in GNRs is comprehensively studied.

Electrons in π bonds of p_z-orbitals in graphene are responsible for electronic conduction. In this work, a first nearest-neighbor tight-binding model is employed to describe the electronic bandstructure of GNRs. The hopping parameter between first nearest-neighbor carbon atoms is assumed to be -2.7 eV. Surface corrugations, however, change the bonding lengths between carbon atoms which significantly modulate the hopping parameters. Based on the Harrison's model, the hopping parameter is inversely proportional to the square of the bonding length $t \propto 1/l^2$.[12] Using this model, the effect of the substrate corrugation, which affects the bonding lengths between carbon atoms, on the hopping parameter and as a result the electronic properties of GNRs is investigated. Small bending of p_z-orbitals due to corrugation need to be considered, but it has been shown that the modulation of the hopping parameters due to the bonding length variation is much stronger than that of orbital bending.[13]

Surface corrugation of the substrate is an statistical phenomena which can be modeled by a Gaussian auto-correlation function (ACF)[4–6,14]

$$R(x,y) = \delta h^2 \exp\left(-\frac{x^2}{{L_x}^2} - \frac{y^2}{{L_y}^2}\right), \tag{1}$$

where L_x and L_y are the roughness correlation lengths along the x and y-direction, respectively, which indicate the distance at which corrugation is relatively repeated and δh is the root mean square of the fluctuation amplitude and is an indication of the fluctuations height. The related parameters for various substrate materials are mentioned in Table I.

To generate surface corrugation in spatial domain, the auto-correlation function is Fourier transformed to obtain the spectral function. A random phase with even parity is applied and followed by an inverse Fourier transformation.[15] For the given geometrical and roughness parameters, many samples are created and the electronic characteristics of each sample is evaluated. By taking an ensemble average, the role of corrugation parameters on the average device characteristics is investigated. The non-equilibrium Green's function (NEGF) method is employed in this work to study transport of carriers in GNRs. Details of our approach are described in Ref. 15.

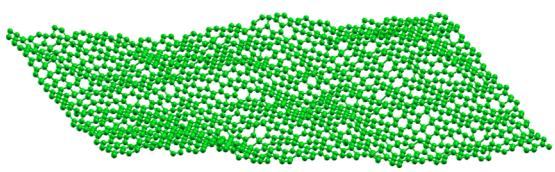

FIG. 1. 3D sketch of a corrugated AGNR.

a)Electronic addresses: pourfath@ut.ac.ir and pourfath@iue.tuwien.ac.at

TABLE I. Surface corrugation parameters for various substrate materials, see Refs. 4–7.

	SiO_2	Boron-nitride	Mica
δh	168–360 pm	$\simeq$ 75pm	24 pm
$L_x = L_y$	15–32 nm	–	2 nm

Depending on the material type and cleaning process, the corrugation amplitude and correlation length can approximately vary between 24–340 pm and 2–32 nm, respectively, see Table I. The average transmission probability as a function of energy at various δh for an AGNR and a zigzag graphene nanoribbon (ZGNR) are shown in Figs. 2(a) and 2(b), respectively. As δh increases, the transmission probability decreases due to increased carrier scattering rate. Subbands can be recognized for small values of δh (small perturbation). At large values of δh, steps in the transmission probability are smoothed out. On the other hand, the average transmission probability increases with the correlation length, see Fig. 2(c) for AGNR and Fig. 2(d) for ZGNR. As the correlation length increases, surface corrugation becomes smoother which leads to the reduction of carrier scattering rate.

In the absence of scattering, the transmission probability is independent of the channel length. However, the transmission has an inverse proportionality to the channel length in the presence of scattering

$$T(E) = N_{\mathrm{ch}}(E)/(1 + L/\lambda(E)), \tag{2}$$

where $\lambda(E)$ is defined as the MFP of carriers. To quantify the role of surface corrugation on the electronic properties of GNRs, the MFPs as functions of the corrugation amplitude and correlation length are extracted. For this purpose, at each energy, a curve based on Eq. (2) is fitted to the average transmission probability as a function of the channel length (Fig. 3(a)) and the respective MFP at that particular energy is extracted, see Fig. 3(b). The MFP increases at each subband with energy but it falls down at the edge of the next subband. A van-hove singularity appears at the edge of each subband which results in significant increase of the density of state and scattering rate of carriers, therefore, the MFP decreases at these edges. Because of the absence of such van-hove singularities in the electronic bandstructure of graphene, one should expect that the surface corrugation plays a more important role on the electronic properties of GNRs than that of graphene.

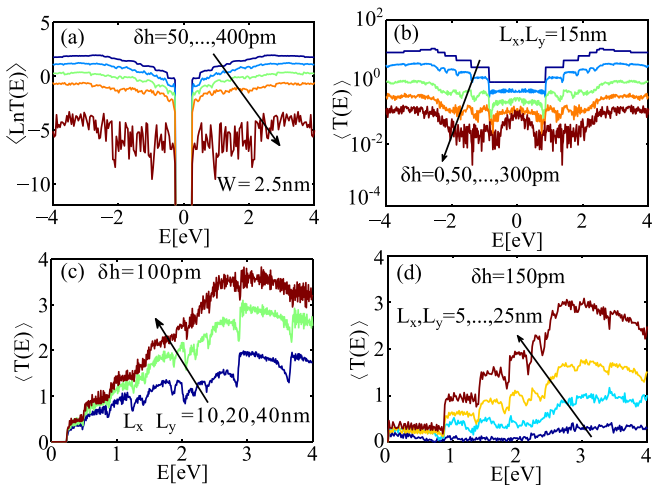

FIG. 2. The average transmission probability as a function of energy at various corrugation amplitudes and $L_x = L_y = 25$nm for the (a) AGNR and (b) ZGNR. The average transmission probability as a function of energy at various correlation lengths for the (c) AGNR with $\delta h = 50$ pm and (d) ZGNR with $\delta h = 150$ pm. $W = 2.5$ nm for both the AGNR and ZGNR and $L = 100$ nm for the AGNR and $L = 50$ nm for the ZGNR.

Figs. 4(a) and 4(b) indicate the MFP scales with corrugation amplitude as δh^{-4} for both the AGNR and ZGNR, respectively, whereas MFP scales linearity with the correlation length, see Figs. 4(c) and 4(d) for AGNR and ZGNR, respectively. It should be noted that the relatively larger MFP of the ZGNR, in comparison with that of the AGNR, is due to the robustness of edge-states against disorder in zigzag configuration[16] (see the inset of Fig. 4(b)). As the correlation length increases, surface corrugation becomes smoother, and the scattering rate is reduced. The scaling of MPF with the corrugation amplitude can be approximated from the Fermi golden rule. The bonding length in the presence of surface corrugation can be expressed as $l^2 = a_{cc}^2 + \Delta h_{ij}^2$ where Δh_{ij} is the height difference between two nearest neighbor atoms and a_{cc} is the distance between nearest neighbor carbon atoms in graphene. Assuming $h_{ij} \ll a_{cc}$, one can employ Harrison's[12] model to approximate the hopping parameters with

$$t_{ij} = t_0 \frac{1}{(l_{ij}/a_{cc})^2} = \frac{t_0}{1 + \Delta h_{ij}^2/a_{cc}^2} \simeq t_0 \left(1 - \frac{\Delta h_{ij}^2}{a_{cc}^2}\right). \tag{3}$$

Therefore, the modulation of the hopping parameter is quadratically proportional to corrugation amplitude $\delta t_{ij} \propto \Delta h_{ij}^2$ and one obtains $\langle i|\delta H|j\rangle = \delta t_{ij} \propto \Delta h_{ij}^2$. Taking an ensemble average over hopping parameters yields

$$\begin{aligned} \langle \delta t \rangle \propto \langle \Delta h_{ij}^2 \rangle &= \langle |h(x,y) - h(x + a_{cc}, y)|^2 \rangle \\ &= \langle h(x,y)^2 \rangle + \langle h(x + a_{cc}, y)^2 \rangle \\ &\quad - 2\langle h(x,y) h(x + a_{cc}, y) \rangle, \end{aligned} \tag{4}$$

considering that $\langle h(x,y)h(x+x', y+y')\rangle$ is defined as the ACF of roughness amplitude, $\langle h(x,y)^2\rangle = \langle h(x+a_{cc},y)^2\rangle = \delta h^2$ and $\langle h(x,y)h(x+a_{cc},y)\rangle = \delta h^2 \exp(-a_{cc}^2/L_x^2)$. As a result, $\langle \delta t \rangle \propto \delta h^2$. Based on the Fermi golden rule, the scattering rate due to surface roughness is given by τ^{-1}

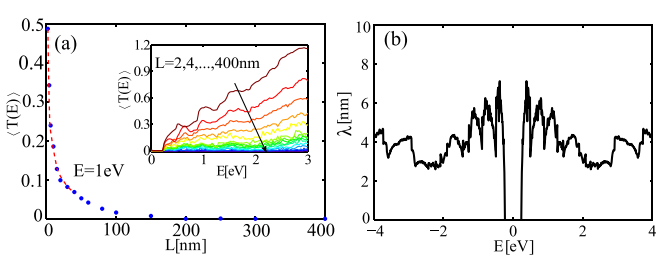

FIG. 3. (a) The average transmission probability as a function of length at $E = 1$ eV for $\delta h = 250$ pm. The dashed-line is a fitted curve based on Eq. (2) for extracting the MFP. (b) The MFP as a function of energy for $\delta h = 150$ pm. All results are for the AGNR with $W = 2.5$ nm and $L_x = L_y = 15$nm.

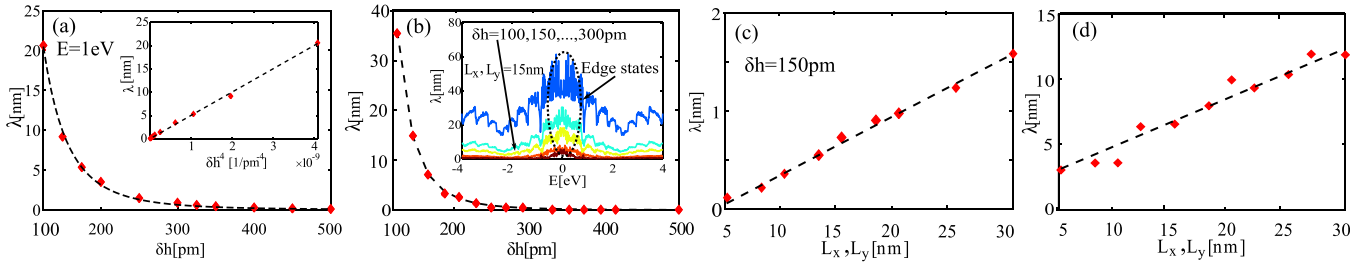

FIG. 4. The dependency of the MFP with the corrugation amplitude at $L_x = L_y = 15$nm for the (a) AGNR with $W = 5$ nm and the (b) ZGNR with $W = 3$ nm. The symbols indicate simulation results and the dashed curves are fitted lines based on $\lambda \propto \delta h^{-4}$. The inset of Fig. 4(a) shows the MFP as a function of h^{-4}. The inset of Fig. 4(b) depicts the MFP as a function of energy for the ZGNR. Relatively large MFPs close to the Dirac point are due to the robustness of the edge states og ZGNR against disorder. The dependency of the MFP with the correlation length for the (c) AGNR with $W = 2.5$ nm, $\delta h = 150$ pm and (d) ZGNR with $W = 3$ nm and $\delta h = 150$ pm. The symbols are the simulation results and the dashed curves are fitted to $\lambda \propto L_x, L_y$. All MFPs in (a)–(d) are extracted at E = 1 eV.

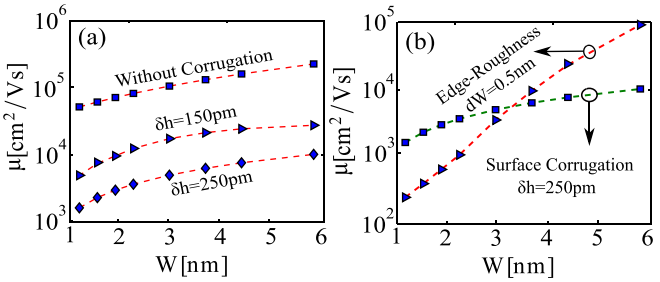

FIG. 5. (a) The mobility of the AGNR as a function of width at various corrugation amplitudes. (b) A comparison between the role of surface corrugation amplitude and that of line-edge roughness on the mobility as a function of the ribbon's width. $L_x = L_y = 15$ nm and $L = 50$ nm.

$\propto |\langle i|\delta H|j\rangle|^2 = |\langle \delta t\rangle|^2 \propto \delta h^4$. The MFP, therefore, scales with corrugation amplitude as $\lambda \propto 1/\delta h^4$.

Next, we investigate the role of surface corrugation on the mobility of AGNRs. Mobility can be evaluated from $\mu(E) = \sigma(E)/n$,[17] in which n is the electron concentration and $\sigma(E)$ is the conductivity that can be obtained based on linear response theory $\sigma(E) = (2q^2/h)T(E)(-\partial f(E)/\partial E)$, with f as the Fermi-Dirac distribution function. Fig. 5(a) shows mobility as a function of width at various corrugation amplitudes. The results indicate that the mobility is considerably degraded for corrugation amplitudes around 250 pm, which is a typical value for SiO_2 substrates. Fig. 5(b) compares the role of edge roughness and surface corrugation on the mobility of AGNR placed on a SiO_2 substrate. The details of edge roughness limited mobility evaluation are described in Ref. 18. Although edge roughness is the most detrimental scattering mechanism on the electronic properties of narrow AGNRs, surface corrugation appears as a dominant scattering mechanism for AGNRs with widths wider than approximately 3 nm placed on SiO_2 substrates.

The role of surface corrugation on the electronic properties of GNRs is theoretically investigated, employing an atomistic tight-binding model along with the NEGF formalism. The dependency of the MFP on the corrugation amplitude and correlation length is studied. The results indicate that MFP scales with the corrugation amplitude as $\lambda \propto \delta h^{-4}$, whereas it scales linearity with the correlation length. The importance of considering surface corrugation on the analysis of narrow GNRs on SiO_2 substrates is also investigated.

[1]K. I. Bolotin, K. J. Sikes, J. Hone, H. L. Stormer, and P. Kim, Phys. Rev. Lett. **101**, 096802 (2008).
[2]M. Katsnelson and A. Geim, Philos. Trans. R. Soc. London, Ser. A **366**, 195 (2008).
[3]J. C. Meyer, A. K. Geim, M. I. Katsnelson, K. S. Novoselov, T. J. Booth, and S. Roth, Nature **446**, 60 (2007).
[4]C. H. Lui, L. Liu, K. F. Mak, G. W. Flynn, and T. F. Heinz, Nature **462**, 339 (2009).
[5]M. Ishigami, J. H. Chen, W. G. Cullen, M. S. Fuhrer, and E. D. Williams, Nano Lett. **7**, 1643 (2007).
[6]V. Geringer, M. Liebmann, T. Echtermeyer, S. Runte, M. Schmidt, R. Rückamp, M. Lemme, and M. Morgenstern, Phys. Rev. Lett. **102**, 76102 (2009).
[7]C. Dean, A. Young, I. Meric, C. Lee, L. Wang, S. Sorgenfrei, K. Watanabe, T. Taniguchi, P. Kim, K. Shepard *et al.*, Nat. Nanotechnol. **5**, 722 (2010).
[8]A. Fasolino, J. H. Los, and I. Katsnelson, Nature Mater. **6**, 858 (2007).
[9]S. V. Morozov, K. S. Novoselov, M. I. Katsnelson, F. Schedin, D. C. Elias, J. A. Jaszczak, and A. K. Geim, Phys. Rev. Lett. **100**, 016602 (2008).
[10]S. Koenig, N. Boddeti, M. Dunn, and J. Bunch, Nat. Nanotechnol. **6**, 543 (2011).
[11]S. Costamagna, O. Hernandez, and A. Dobry, Phys. Rev. B **81**, 115421 (2010).
[12]W. A. Harrison, *Elementary Electronic Structure* (World Scientific Publishing Company, River Edge, NJ, 1999).
[13]J. W. Klos, A. A. Shylau, I. V. Zozoulenko, H. Xu, and T. Heinzel, Phys. Rev. B **80**, 245432 (2009).
[14]S. Goodnick, D. Ferry, C. Wilmsen, Z. Liliental, D. Fathy, and O. Krivanek, Phys. Rev. B **32**, 8171 (1985).
[15]A. Yazdanpanah, M. Pourfath, M. Fathipour, H. Kosina, and S. Selberherr, IEEE Trans. Electron Devices **59**, 433 (2012).
[16]D. A. Areshkin, D. Gunlycke, and C. T. White, Nano Lett. **7**, 204 (2007).
[17]A. Lherbier, B. Biel, Y. Niquet, and S. Roche, Phys. Rev. Lett. **100**, 036803 (2008).
[18]A. Y. Goharrizi, M. Pourfath, M. Fathipour, H. Kosina, and S. Selberherr, IEEE Trans. Electron Devices **58**, 3725 (2011).